

OSCILLATIONS OF ELECTRON–HOLE PLASMA IN TERAHERTZ EMITTERS

A. Reklaitis

Semiconductor Physics Institute, Center for Physical Sciences and Technology, A. Goštauto 11, LT-01108 Vilnius, Lithuania
E-mail: reklaitis@pfi.lt

Received 28 July 2015; accepted 29 September 2015

Oscillations of photogenerated electron–hole plasma in freestanding terahertz emitters are studied using the hydrodynamic analysis and Monte Carlo simulations. The pronounced plasma oscillations are obtained in an *n*-GaAs emitter in which the oscillations are initiated by the surface electric field. The plasma oscillations are also found in an *n*-InAs emitter in which the oscillations are induced by the photo-Dember effect.

Keywords: optical excitation, plasma oscillations, GaAs, InAs

PACS: 52.65.Pp, 73.50.Mx, 73.50.Pz

1. Introduction

Instabilities of charge carriers in semiconductors may arise as a result of several physical phenomena [1]. The plasma instability of electrons may develop when the electron momentum distribution becomes inverted in high electric fields [2]. The plasma instability may be also excited in the appropriately designed semiconductor structures in which the quasiballistic transport conditions are realized [3]. The experimental observation of plasma instabilities in semiconductors in high electric fields is difficult. The main difficulties are associated with the damping of plasma oscillations by the intense phonon and impurity scattering. On the other hand, the frequency of electron–hole plasma oscillations in semiconductors lies in the THz frequency range. Therefore, along with other methods of generation of THz radiation – selective thermal stimulation [4, 5] and photomixing [6, 7], the excitation of plasma oscillations is very attractive for THz technology.

The plasma oscillations in semiconductors may develop when the electron–hole pairs are generated by the femtosecond optical pulse. The optically generated electrons and holes are accelerated in opposite directions by the built-in electric field. The separated

carriers induce the restoring electric field which attracts the electrons and holes. As a result, the oscillations of electron–hole plasma originate. The rapid progress in THz technology over the past two decades [8–10] offered an opportunity for a direct observation of the optically generated electron–hole plasma oscillations from the time-resolved measurements of THz emission. However, the temporal waveforms of THz radiation observed in most experimental studies evidence the onset of a single current surge and do not indicate the development of plasma oscillations [11–14]. Several attempts have been made to detect the oscillations of electron–hole plasma generated by the femtosecond optical pulse. The two non-pronounced periods of plasma oscillations were observed in the *p-i-n* structure from electro-absorption measurements [15] and in *n*-GaAs from time-resolved measurements of THz radiation [16]. Similar results were obtained from reflectivity measurements in GaAs Schottky diodes [17].

In this work, the excitation of plasma oscillations of photogenerated carriers by the surface electric field in homogeneously doped *n*-GaAs is investigated. It is shown that plasma oscillations can be also excited by the photo-Dember effect in *n*-InAs. The dynamics of the oscillations of photogenerated carriers is analyzed

using the hydrodynamic model and ensemble Monte Carlo (EMC) simulations.

2. Models of GaAs and InAs emitters

The semiclassical motion of extrinsic and photogenerated carriers in freestanding THz emitters is simulated by the EMC method. The spatio-temporal variation of electric field is obtained from the solution of the Poisson equation which is self-consistently coupled with the instant space charge distribution of electrons, holes, and ionized impurities. The simulations are performed in a one-dimensional real space and in a three-dimensional momentum space. The one-dimensional real space approach is a good approximation as long as the size of the laser beam is significantly larger than the absorption depth. The details of the applied EMC method as well as the simulation of the photogeneration are given elsewhere [18].

The models of the conduction band structure of GaAs and InAs consisting of nonparabolic Γ , L , and X valleys are considered in the simulations. For the valence band, heavy, light, and split-off nonparabolic subbands are taken into account. The band structure and material parameters for GaAs and InAs are taken the same as in [19] and [20], respectively. The electron scattering mechanisms considered in the simulations include polar optical, inelastic deformation acoustic, intervalley, and ionized impurity scattering, as well as electron–electron and electron–hole interactions. The interaction of holes with polar optical phonons, deformation optical and acoustic phonons is considered for intrasubband and intersubband scattering of holes taking into account the overlap between p -like wave functions of the valence band. The ionized impurity scattering as well as the hole–hole and hole–electron interactions are also taken into account. The calculations are carried out for lattice temperature of 300 K.

The thickness of the simulated n -GaAs and n -InAs structures is 1000 nm. The doping densities in n -GaAs and n -InAs structures are 10^{16} cm^{-3} and $2 \times 10^{17} \text{ cm}^{-3}$, respectively. The electron–hole pairs are excited with the Gaussian optical pulse. The full width at half maximum of the optical pulse is set to 10 fs in EMC simulations. The central photon energy is 1.55 eV. At this photon energy, the light absorption coefficients α in GaAs and InAs are $1.25 \times 10^4 \text{ cm}^{-1}$ [21] and $7.0 \times 10^4 \text{ cm}^{-1}$ [22], respectively.

3. Oscillations induced by the surface field

The equilibrium profile of the conduction and valence bands in n -GaAs (see Fig. 1) is determined by the sur-

face Fermi level F_s which is pinned at the middle of the energy band-gap, i. e. 0.71 eV below the conduction band edge [23]. The surface Fermi level and the doping density control the built-in electric field, the strength of which is 41 kV/cm at the surface of n -GaAs doped to 10^{16} cm^{-3} . The built-in electric field accelerates the photogenerated electrons and holes and initiates plasma oscillations which are damped by the phonon and impurity scattering. The intensity and spectrum of the resulting THz radiation are determined by the temporal derivative of the electric dipole moment of the THz emitter. The temporal derivative of the electric dipole moment is given by the total photocurrent which is obtained by integrating the electron and hole current densities over the thickness of the simulated structure.

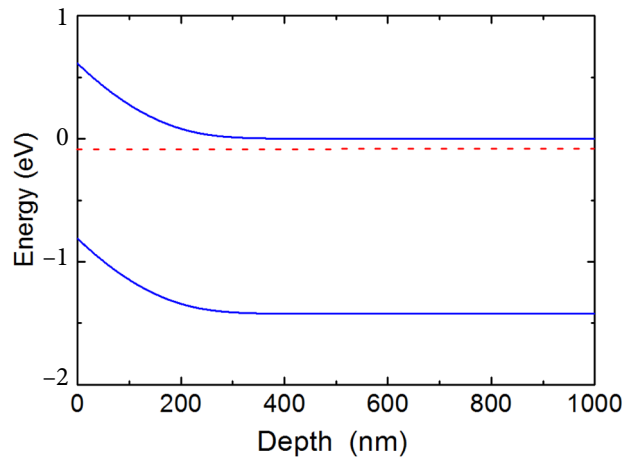


Fig. 1. Equilibrium potential profile (conduction and valence band edges) in n -GaAs doped to 10^{16} cm^{-3} . The Fermi level is shown by the dashed line.

The hydrodynamic model of the photogenerated plasma in p - i - n structures with a uniform built-in electric field is developed in [24]. The hydrodynamic model of [24] can be generalized to treat the position-dependent surface electric field problem. The solution of Eq. (4) of [24] multiplied by the space charge density of photoexcited carriers gives the position- and time-dependent photocurrent density $j(z, t)$ of electrons and holes as

$$j(z, t) = \frac{e^2 E(z) n_{\text{exc}} \exp(-az)}{[\omega_p^2 - \gamma^2 / 4]^{1/2}} \times \exp(-\gamma t / 2) \times \sin[(\omega_p^2 - \gamma^2 / 4)^{1/2} t], \quad (1)$$

where

$$\omega_p = [e^2 n_{\text{exc}} \exp(-\alpha z) / \kappa \kappa_0 m^*]^{1/2} \quad (2)$$

is the position-dependent plasma frequency of photocarriers, e is the elementary charge, $E(z)$ is the position-dependent built-in electric field, n_{exc} is the density of photogenerated electron–hole pairs at the surface, γ is the momentum relaxation rate of electrons and holes, m^* is the reduced effective mass of electrons and holes, κ is the dielectric permittivity, and κ_0 is the static dielectric constant.

The built-in electric field extends to a distance of $L \approx 250$ nm from the surface of n -GaAs doped to 10^{16} cm $^{-3}$ (see Fig. 1). Hence, the inequality $\alpha L \ll 1$ is satisfied for n -GaAs doped to 10^{16} cm $^{-3}$, and Eq. (1) may be simplified by replacing $\exp(-\alpha z)$ with unity. Then we obtain

$$j(z, t) = \frac{e^2 E(z) v_{\text{exc}} \exp(-\gamma t / 2)}{[\omega_{p0}^2 - \gamma^2 / 4]^{1/2}} \times \sin[(\omega_{p0}^2 - \gamma^2 / 4)^{1/2} t], \quad (3)$$

where

$$\omega_{p0} = [e^2 n_{\text{exc}} / \kappa \kappa_0 m^*]^{1/2} \quad (4)$$

is the plasma frequency at the surface. Integration of Eq. (3) over z yields the total photocurrent (temporal derivative of the electric dipole moment)

$$J(z, t) = \frac{e(F_b - F_s) n_{\text{exc}} \exp(-\gamma t / 2)}{[\omega_{p0}^2 - \gamma^2 / 4]^{1/2}} \times \sin[(\omega_{p0}^2 - \gamma^2 / 4)^{1/2} t], \quad (5)$$

where F_b is the Fermi energy in the bulk. The Fermi energy in the bulk is 0.097 eV below the conduction band edge of n -GaAs doped to 10^{16} cm $^{-3}$.

Equation (5) shows that the near-coherent oscillations of photogenerated electron–hole plasma are excited when the condition $\alpha L \ll 1$ is satisfied. This conclusion is confirmed by the results of rigorous EMC simulations. The comparison of the results given by Eq. (5) with the results of EMC simulations is shown in Fig. 2. The momentum relaxation rate $\gamma = 7 \times 10^{12}$ s $^{-1}$ is taken in Eq. (5). The results shown in Fig. 2 evidence that the dynamics of photoexcited electron–hole plasma is well described by the hydrodynamic model. The obtained from EMC simulations frequency of plasma oscillations increases as the density of photocarriers rises, in agreement with Eqs. (4)

and (5). The Fourier analysis of the transient photocurrent gives the central frequency of oscillations $f = 2.2$ THz when $n_{\text{exc}} = 5 \times 10^{16}$ cm $^{-3}$ and $f = 4.7$ THz when $n_{\text{exc}} = 2.5 \times 10^{17}$ cm $^{-3}$.

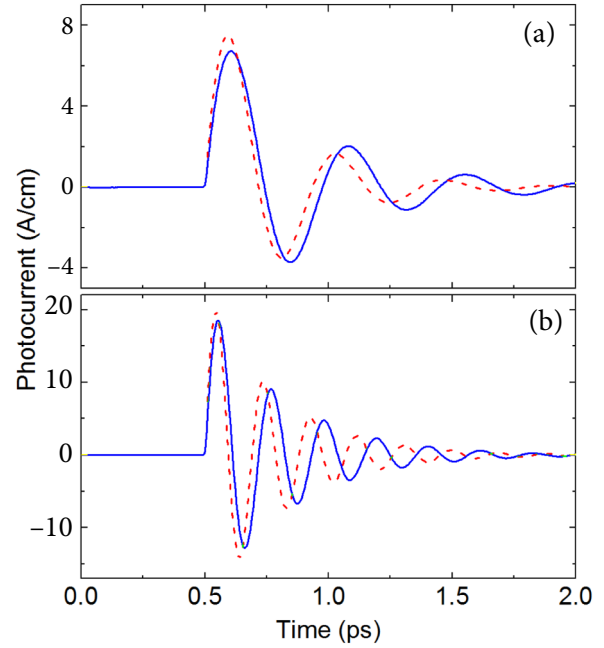


Fig. 2. Total photocurrent in n -GaAs as obtained from EMC simulations (solid curves) and calculated from Eq. (5) (dashed curves). The optical pulse is centered at $t = 0.5$ ps. The results are obtained for the generation densities of 5×10^{16} cm $^{-3}$ (a) and 2.5×10^{17} cm $^{-3}$ (b).

The obtained from EMC simulations temporal evolution of the potential profile is shown in Fig. 3. The dynamics of the potential profile supports the picture of damped plasma oscillations. By $t = 0.4$ ps, the potential profile is in equilibrium. The peak of the optical pulse intensity is at the time moment $t = 0.5$ ps. The created electrons and holes are accelerated in opposite directions. Due to the spatial separation of electrons and holes, the electric field is screened. Then, due to the quasiballistic motion of carriers, the electric field changes its sign. By $t = 0.75$ ps, the electric field reaches its maximum negative value. By $t = 1$ ps, the electric field reaches its maximum positive value during the second period of oscillations. The coherent motion of carriers is dephased by the phonon, impurity and intercarrier scattering. As a result, by $t = 2$ ps, the quasi-equilibrium carrier distribution is established. The motion of electrons and holes is completely dephased, and the built-in electric field is fully screened by the space charge of photogenerated carriers.

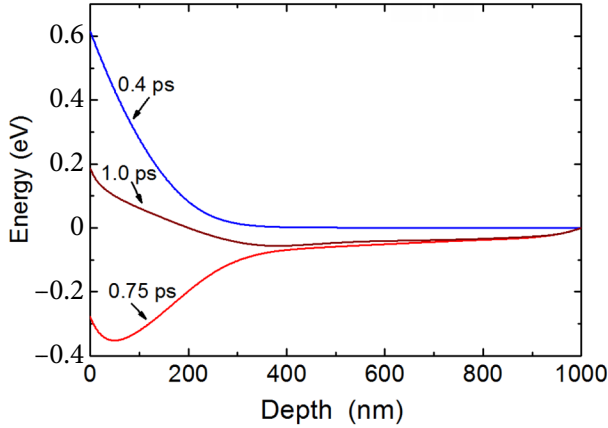


Fig. 3. Snapshots of the potential profile in n -GaAs doped to 10^{16} cm^{-3} at the time moments shown in the figure. The results are obtained from EMC simulations. The optical pulse is centered at $t = 0.5 \text{ ps}$. The generation density is $5 \times 10^{16} \text{ cm}^{-3}$.

The equilibrium state of the emitter after optical pulse is recovered by means of carrier recombination. Several conditions are identified in [25] which have to be fulfilled for the experimental observation of the pronounced oscillations of electron–hole plasma excited by short optical pulses. The results of present simulations indicate that there is an additional constraint for this purpose. The simulated response of the n -GaAs emitter to the series of optical pulses shows that the pronounced plasma oscillations are excited only by the first optical pulse if the time interval between pulses is too short for the complete recombination of photogenerated carriers. The subsequent optical pulses do not excite plasma oscillations because the oscillations are heavily damped by the residual carriers. This fact suggests that the optical pulses with a low repetition rate have to be used for the experimental observation of plasma oscillations. The time interval between the optical pulses must be sufficiently long for the complete recombination of photogenerated carriers.

4. Oscillations initiated by the photo-Dember effect

The dominant mechanism of THz emission from the (100) oriented InAs surface is the transient photocurrent induced by the photo-Dember effect [26, 27]. The surface Fermi level in InAs is pinned at 0.2 eV above the conduction band edge [28]. The position of the surface Fermi level determines the downward band bending of the conduction and valence bands in n -InAs at equilibrium (see Fig. 4).

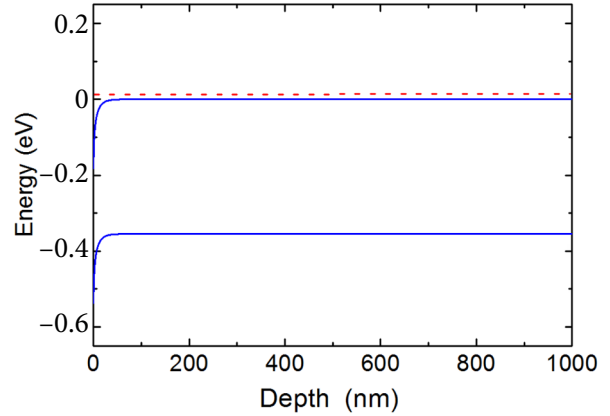


Fig. 4. Equilibrium potential profile (conduction and valence band edges) in n -InAs doped to $2 \times 10^{17} \text{ cm}^{-3}$. The Fermi level is shown by the dashed line.

The downward band bending is neglected in the hydrodynamic model of the photo-Dember effect developed in [20]. It is assumed that the potential is constant throughout the structure prior to photogeneration. This assumption is justified by the fact that the kinetic energy of excited carriers exceeds the energy of electron confinement due to downward band bending. Then, the hydrodynamic model [20] gives the total photocurrent as

$$J(t) = \frac{4\kappa\kappa_0 m^* v_t^2}{e} \times \frac{\exp(-\gamma t / 2)}{t} \times \sin\left(\frac{\omega_{\max} + \omega_{\min}}{2} t\right) \times \sin\left(\frac{\omega_{\max} - \omega_{\min}}{2} t\right), \quad (6)$$

where

$$v_t^2 = v_{te}^2 - v_{th}^2 \quad (7)$$

is the difference between the average squared velocities of the excited electrons, v_{te}^2 , and holes, v_{th}^2 , immediately after photogeneration,

$$\omega_{\max} = (\omega_{\text{exc}}^2 + \omega_{\text{eq}}^2 - \gamma^2 / 4)^{1/2}, \quad (8)$$

$$\omega_{\min} = (\omega_{\text{eq}}^2 - \gamma^2 / 4)^{1/2}, \quad (9)$$

$$\omega_{\text{exc}} = (e^2 n_{\text{exc}} / \kappa\kappa_0 m^*)^{1/2} \quad (10)$$

is the plasma frequency of photogenerated carriers,

$$\omega_{\text{eq}} = (e^2 n_{\text{eq}} / \kappa\kappa_0 m_{\text{eq}})^{1/2} \quad (11)$$

is the plasma frequency of equilibrium electrons, n_{eq} is the equilibrium electron density before photogeneration, m^* is the reduced effective mass of photogenerated carriers, and m_{eq} is the effective mass of equilibrium electrons. At low generation density $n_{\text{exc}} \ll n_{\text{eq}}$, Eq. (6) reduces to

$$J(t) = \frac{en_{\text{exc}}v_t^2 \exp(-\gamma t/2)}{(\omega_{\text{eq}}^2 - \gamma^2/4)^{1/2}} \times \sin[(\omega_{\text{eq}}^2 - \gamma^2/4)^{1/2}t]. \quad (12)$$

In this limit, the frequency of plasma oscillations becomes position-independent, and it is controlled by the density n_{eq} of the uniformly distributed equilibrium electrons.

It follows from Eq. (12) that the hydrodynamic model predicts the excitation of damped plasma oscillations which are induced by the photo-Dember effect. This prediction is verified by EMC simulations. The comparison of the transient photocurrent in n -InAs as obtained from Eq. (6) and from EMC simulations is shown in Fig. 5 at low and high generation densities. The momentum relaxation rate $\gamma = 10^{13} \text{ s}^{-1}$ is taken in Eq. (6). The momentum relaxation in n -InAs doped to $2 \times 10^{17} \text{ cm}^{-3}$ is controlled primarily

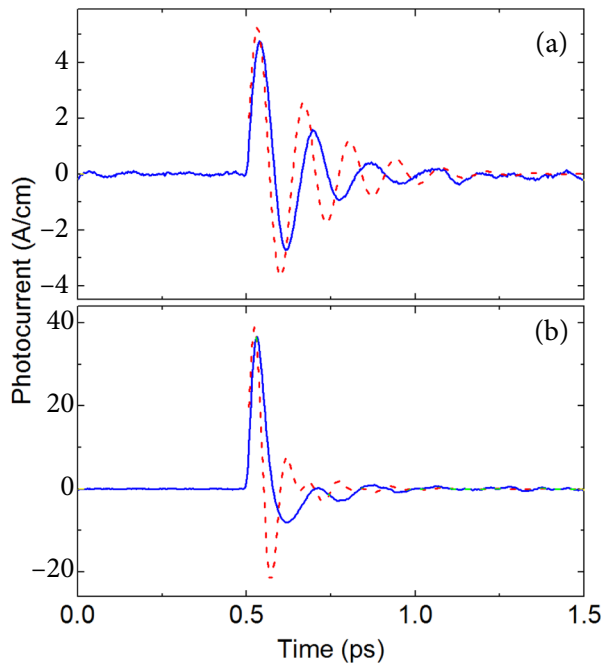


Fig. 5. Total photocurrent in n -InAs as obtained from EMC simulations (solid curves) and calculated from Eq. (6) (dashed curve). The optical pulse is centered at $t = 0.5 \text{ ps}$. The results are obtained for the generation densities of $2.8 \times 10^{17} \text{ cm}^{-3}$ (a) and $2.8 \times 10^{18} \text{ cm}^{-3}$ (b).

by the ionized impurity scattering. The pronounced plasma oscillations are obtained from EMC simulations at low generation density $n_{\text{exc}} = 2.8 \times 10^{17} \text{ cm}^{-3}$ (see Fig. 5(a)). Only one single current surge is obtained at high generation density as seen from Fig. 5(b).

The mechanism of the excitation of plasma oscillations in n -InAs can be understood from the temporal evolution of the potential profile shown in Fig. 6. As seen from the potential profile at $t = 0.58 \text{ ps}$, a strong electric field is developed during the first time moments after photogeneration due to the initial spatial separation of electrons and holes. The initial separation of carriers is induced by different diffusion rates of photogenerated electrons and holes. Then, the strong electric field initiates plasma oscillations. After the first period of oscillations, the potential profile becomes as shown at $t = 0.66 \text{ ps}$. At $t = 1.5 \text{ ps}$, the oscillations are damped, and the quasi-equilibrium state of the electron-hole system is established.

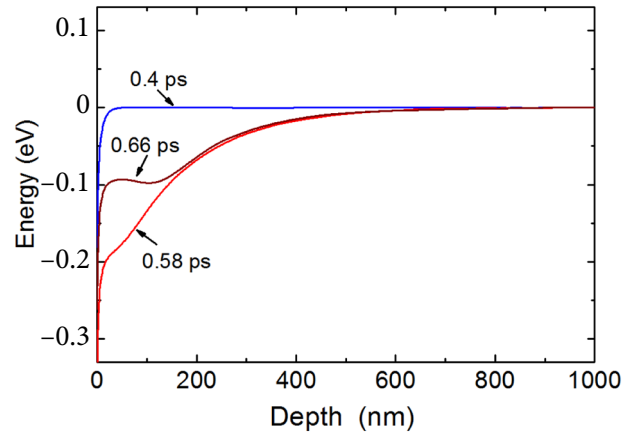


Fig. 6. Snapshots of the potential profile in n -InAs doped to $2 \times 10^{17} \text{ cm}^{-3}$ at the time moments shown in the figure. The results are obtained from EMC simulations. The optical pulse is centered at $t = 0.5 \text{ ps}$. The generation density is $2.8 \times 10^{17} \text{ cm}^{-3}$.

5. Conclusions

The dynamics of electron-hole plasma generated by the femtosecond optical pulse in freestanding THz emitters is investigated using hydrodynamic model and ensemble Monte Carlo simulations. The pronounced and near-coherent plasma oscillations are excited in the n -GaAs emitter when the surface field thickness is less than the absorption depth. The oscillation frequency is determined by the density of excited carriers. The plasma oscillations are also excited in the n -InAs emitter when the density of

photogenerated carriers is low. In this case, the oscillation frequency is controlled by the doping density.

References

- [1] J. Pozhela, *Plasma and Current Instabilities in Semiconductors* (Pergamon, Oxford, 1981).
- [2] Yu. Pozhela and A. Reklaitis, Instability of hot electrons in two-valley semiconductors, *JETP Lett.* **31**(12), 673–676 (1980), www.jetpLetters.ac.ru/ps/1360/article_20546.pdf
- [3] V. Gružinskas, R. Mickevičius, J. Požela, and A. Reklaitis, Collective electron interaction in double-barrier GaAs structures, *Europhys. Lett.* **5**(4), 339–341 (1988), <http://dx.doi.org/10.1209/0295-5075/5/4/010>
- [4] J. Požela, E. Širmulis, K. Požela, A. Šilėnas, and V. Jucienė, SiC and GaAs emitters as selective terahertz radiation sources, *Lith. J. Phys.* **53**(3), 163–167 (2013), <http://dx.doi.org/10.3952/lithjphys.53306>
- [5] K. Požela, E. Širmulis, I. Kašalynas, A. Šilėnas, J. Požela, and V. Jucienė, Selective thermal terahertz emission from GaAs and AlGaAs, *Appl. Phys. Lett.* **105**(9), 091601 (2014), <http://dx.doi.org/10.1063/1.4894539>
- [6] S. Preu, G.H. Döhler, S. Malzer, L.J. Wang, and A.C. Gossard, Tunable, continuous-wave terahertz photomixer sources and applications, *J. Appl. Phys.* **109**(6), 061301 (2011), <http://dx.doi.org/10.1063/1.3552291>
- [7] G. Seniutinas, G. Gervinskas, E. Constable, A. Krotkus, G. Molis, G. Valušis, R.A. Lewis, and S. Juodkazis, THz photomixer with milled nanoelectrodes on LT-GaAs, *Appl. Phys. A* **117**(2), 439–444 (2014), <http://dx.doi.org/10.1007/s00339-014-8685-8>
- [8] A. Krotkus, Semiconductors for terahertz photonics applications, *J. Phys. D* **43**(27), 273001 (2010), <http://dx.doi.org/10.1088/0022-3727/43/27/273001>
- [9] R.A. Lewis, A review of terahertz sources, *J. Phys. D* **47**(37), 374001 (2014), <http://dx.doi.org/10.1088/0022-3727/47/37/374001>
- [10] V. Apostolopoulos and M.E. Barnes, THz emitters based on the photo-Dember effect, *J. Phys. D* **47**(37), 374002 (2014), <http://dx.doi.org/10.1088/0022-3727/47/37/374002>
- [11] M. Nakajima, M. Hangyo, M. Ohta, and H. Miyazaki, Polarity reversal of terahertz waves radiated from semi-insulating InP surfaces induced by temperature, *Phys. Rev.* **67**(19), 195308 (2003), <http://dx.doi.org/10.1103/PhysRevB.67.195308>
- [12] J.N. Heyman, N. Coates, A. Reinhardt, and G. Strasser, Diffusion and drift in terahertz emission at GaAs surfaces, *Appl. Phys. Lett.* **83**(26), 5476–5478 (2003), <http://dx.doi.org/10.1063/1.1636821>
- [13] S. Winnerl, S. Sinning, T. Dekorsy, and M. Helm, Increased terahertz emission from thermally treated GaSb, *Appl. Phys. Lett.* **85**(15), 3092–3094 (2004), <http://dx.doi.org/10.1063/1.1805197>
- [14] Y. Shi, X. Xu, Y. Yang, W. Yan, S. Ma, and L. Wang, Anomalous enhancement of terahertz radiation from semi-insulating GaAs surfaces induced by optical pump, *Appl. Phys. Lett.* **89**(8), 081129 (2006), <http://dx.doi.org/10.1063/1.2338805>
- [15] W. Sha, A.L. Smirl, and W.F. Tseng, Coherent plasma oscillations in bulk semiconductors, *Phys. Rev. Lett.* **74**(21), 4273–4276 (1995), <http://dx.doi.org/10.1103/PhysRevLett.74.4273>
- [16] R. Kersting, K. Unterrainer, G. Strasser, H.F. Kaufmann, and E. Gornik, Few-cycle THz emission from cold plasma oscillations, *Phys. Rev. Lett.* **79**(16), 3038–3041 (1997), <http://dx.doi.org/10.1103/PhysRevLett.79.3038>
- [17] W. Fischler, P. Buchberger, R.A. Höpfel, and G. Zandler, Ultrafast reflectivity changes in photoexcited GaAs Schottky diodes, *Appl. Phys. Lett.* **68**(20), 2778–2780 (1996), <http://dx.doi.org/10.1063/1.116604>
- [18] A. Reklaitis, Monte Carlo analysis of terahertz oscillations of photoexcited carriers in GaAs *p-i-n* structures, *Phys. Rev. B* **74**(16), 165305 (2006), <http://dx.doi.org/10.1103/PhysRevB.74.165305>
- [19] A. Reklaitis and L. Reggiani, Monte Carlo study of shot-noise suppression in semiconductor heterostructure diodes, *Phys. Rev. B* **60**(16), 11683–11693 (1999), <http://dx.doi.org/10.1103/PhysRevB.60.11683>
- [20] A. Reklaitis, Terahertz emission from InAs induced by photo-Dember effect: Hydrodynamic analysis and Monte Carlo simulations, *J. Appl. Phys.* **108**(5), 053102 (2010), <http://dx.doi.org/10.1063/1.3467526>
- [21] R. Kersting, J.N. Heyman, G. Strasser, and K. Unterrainer, Coherent plasmons in *n*-doped GaAs, *Phys. Rev. B* **58**(8), 4553–4559 (1998), <http://dx.doi.org/10.1103/PhysRevB.58.4553>
- [22] D.E. Aspnes and A.A. Studna, Dielectric functions and optical parameters for Si, Ge, GaP, GaAs, GaSb, InP, InAs, and InSb from 1.5 to 6.0 eV, *Phys. Rev. B* **27**(2), 985–1009 (1983), <http://dx.doi.org/10.1103/PhysRevB.27.985>
- [23] T. Dekorsy, T. Pfeifer, W. Kütt, and H. Kurz, Subpicosecond carrier transport in GaAs surface-space-charge fields, *Phys. Rev. B* **47**(7), 3842–3849 (1993), <http://dx.doi.org/10.1103/PhysRevB.47.3842>
- [24] A. Reklaitis, Coherence of terahertz emission from photoexcited electron–hole plasma: Hydrodynamic model and Monte Carlo simulations, *Phys. Rev. B* **77**(15), 153309 (2008), <http://dx.doi.org/10.1103/PhysRevB.77.153309>
- [25] A. Reklaitis, Theoretical analysis of conditions for observation of plasma oscillations in semiconductors from pulsed terahertz emission, *J. Appl. Phys.* **116**(8), 083107 (2014), <http://dx.doi.org/10.1063/1.4894163>

- [26] K. Liu, J. Xu, T. Yuan, and X.-C. Zhang, Terahertz radiation from InAs induced by carrier diffusion and drift, *Phys. Rev. B* **73**(15), 155330 (2006), <http://dx.doi.org/10.1103/PhysRevB.73.155330>
- [27] E. Estacio, H. Sumikura, H. Murakami, M. Tani, N. Sarukura, M. Hangyo, C. Ponseca Jr., R. Pobre, R. Quiroga, and S. Ono, Magnetic-field-induced fourfold azimuthal angle dependence in the terahertz radiation power of (100) InAs, *Appl. Phys. Lett.* **90**(15), 151915 (2007), <http://dx.doi.org/10.1063/1.2721385>
- [28] L.Ö. Olsson, C.B.M. Andersson, M.C. Håkansson, J. Kanski, L. Ilver, and U.O. Karlsson, Charge accumulation at InAs surfaces, *Phys. Rev. Lett.* **76**(19), 3626–3629 (1996), <http://dx.doi.org/10.1103/PhysRevLett.76.3626>

ELEKTRONŲ IR SKYLIŲ PLAZMOS OSCILIACIJOS TERAHERCINIUOSE EMITERIUOSE

A. Reklaitis

Puslaidininkų fizikos institutas, Fizinių ir technologijos mokslų centras, Vilnius, Lietuva

Santrauka

Panaudojant hidrodinaminį modelį bei modeliavimą Monte Karlo metodu, ištirtos optiškai sukurtų elektronų ir skylių plazmos osciliacijos bekontakčiuose terahercinės spinduliuotės emiteriuose. Gautos ryš-

kiai išreikštos plazminės osciliacijos n -GaAs emiteryje, kuriame osciliacijos yra inicijuotos paviršiniu elektriniu lauku. Plazminės osciliacijos taip pat yra aptiktos n -InAs emiteryje, kuriame osciliacijos yra sukuriamos foto-Demberio efektu.